Reconstruction of Multi-channel MR Magnitude and Phase Images Using Dual-echo Sequence at 7 Tesla

C. Moon[1], and K. Bae[1,2]

[1]Radiology, University of Pittsburgh, Pittsburgh, PA, United States, [2]Bioengineering, University of Pittsburgh, Pittsburgh, PA, United States

[Introduction] The high-field magnet has many potential advantages in human brain imaging (e.g., high SNR, CNR, & high-resolution) [1,2]. And better SNR can be achieved with the multi-channel surface coil and high-field [3,4]. However, B1-inhomogeneity and coupling between the coils and object increase at the high field [5]. As a result, the undesirable artifacts such as intensity inhomogeneity or phase dislocation could appear in magnitude and phase image, respectively. Although a couple of methods [6–8] were suggested to correct the intensity inhomogeneity in magnitude image, other side artifacts could be produced, or the extra scanning and co-registration is required. On the other hand, in the reconstructed susceptibility phase image, the phase noise and dislocation is problematic due of the phase incoherence between the channels and large local field inhomogeneity. In this study, we developed the highly efficient reconstruction algorithm for magnitude and phase image using dual-echo sequence at 7T.

[Methods] All scans were performed on 7T scanner (Siemens Medical Solutions, Erlangen, Germany) with 9-channel (1 volume transceiver + 8 receivers) RF coil. A volunteer consented to the study approved by the IRB of the university. Dual-echo 2D GRE sequence was used to calculate the '*coil sensitivity map*' and '*system phase map*' (Fig. 1). (1) The coil sensitivity map of each channel was generated by compensating T2* effect remaining at PD-weighted 1st echo (and the tissue contrast was low-pass filtered), and combined with other multi-channel data using the root-square-of-sum (RSS) method [9] (Fig. 2). Then, the T2* magnitude image was generated from the T2*-weighted 2nd echo using the RSS method (Fig. 3B), and was masked with the combined coil sensitivity map (Fig. 3C). (2) The acquired phase image of j^{th} channel can be modeled by $\theta_j(x,y) = \theta^{sus}(x,y) + \theta^{inh}(x,y) + \theta_j^{sys}(x,y) + \sigma_j(x,y)$, where $\theta^{sus}(x,y)$ is the (coil-independent) '*susceptibility*' phase that we want to know, $\theta_j^{sys}(x,y)$ is the (coil-dependent) '*system*' phase, $\theta^{inh}(x,y)$ is the (coil-independent) '*macroscopic inhomogeneity*' phase, and $\sigma_j(x,y)$ is the noise term depending on each channel's receiver. The phase of inhomogeneity field $\theta^{sus}(x,y) + \theta^{inh}(x,y)$ can be calculated from the linear relationship of two echoes at different TE, and the system phase $\theta_j^{sys}(x,y)$ can be calculated easily from the above phase model. The calculated system phase was low-pass filtered to remove the noise (120×120 Hamming), and the calculated system phase was subtracted from the measured phase $\theta_j(x,y)$ for each channel. The calculated phase can be directly combined in phase domain and high-pass filtered to make the integrated susceptibility phase image $\theta^{sus}(x,y)$, or can be used for more advanced following reconstruction. The noises in phase map can be removed by the magnitude-weighting with coil sensitivity map, and high-pass filtering before combining all channel's data in complex domain. The calculated susceptibility phase map can be further processed to enhance the local susceptibility such as in the deoxygenated vessels or iron-deposit brain nuclei, and to remove the remaining macroscopic inhomogeneity and system phases. In this study, we applied a high-pass filter with 41×41 Hamming window.

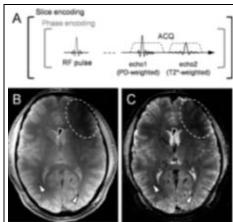

Fig. 1 (A) Dual-echo GRE sequence, (B) 1st echo and (C) 2nd echo MR image each; TR/TE1/TE2 = 2300/5.0/22.4 ms, and BW_1/BW_2 = 160/30 Hz/px Black-arrowhead - lateral body filled with CSF & white-arrowheads vessels, optic radiation. The white-dotted oval region represents the area of dark intensity due to B_1-inhomogeneity and inhomogeneous coil sensitivity. Note that, although the dual-echo images differ in the tissue-contrast, they are similar in their intensity inhomogeneity across whole imaging field.

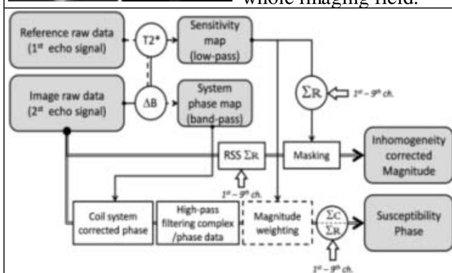

Fig. 2 Estimation of coil sensitivity and system phase map from the dual-echo. The coil sensitivity map was computed with the T2* effect compensation and low-pass filtering from 1st echo, while the system phase map from 1st echo was generated with susceptibility & macroscopic inhomogeneity using the dual-echo. The calculated phase map at each stage was unwrapped using fast-Fourier-transform (FFT) method [10].

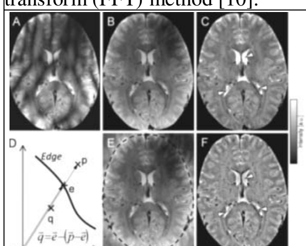

Fig. 3 Magnitude images. (A) Simple-complex-summation. (B) Root-square-summation. (C) Intensity inhomogeneity correction using coil sensitivity map. (D) Schemes of background-filling. To fill the background, first the edge of brain periphery is detected manually or automatically, the center point is calculated for the closed loop of brain boundary (point 'o'), and the edge point (point 'e') is co-aligned with vector (vector 'op') from center to the pixel in background was selected. The pixel in brain (point 'q') is selected at same distance from edge point with distance (vector 'pe') from edge to current background point, and the intensity at chosen pixel is copied to the background point, 'p'. (E) Background-filled image. (F) Intensity inhomogeneity correction using a high-pass filter (10×10 Hamming). Note that excessive high-pass filtering reduces the contrast in large structures in the brain (white-arrowheads in F).

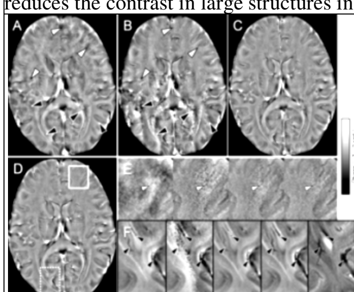

Fig. 4 Phase images. (A) SUP (I-1). White-arrowheads indicate the system phase noise artifacts and overlaid in B. (B) SC (I-2). Black-arrowheads indicate the artifacts due to phase incoherence between channels and overlaid in A. (C) CSMW (II-1). (D) CSSW (II-2). (E) Magnified phase maps of A to D in the white-box in D. White-arrowheads indicate a noise region. (F) Magnified phase maps of A to D and corrected magnitude image in the dotted white box in D. Black-arrowheads indicates venous vessels.

[Results and Conclusions] (1) *Magnitude reconstruction* - The simple summation of raw complex data produced the severe fringe artifacts because of the phase incoherence between the channels (Fig. 3A). The RSS method can compensate an incoherent phase between the channels by neglecting all the phase information, but cannot correct the coil-sensitivity-dependent variation in the imaging space (see the right frontal hemisphere in Fig. 3B). This inhomogeneous intensity was removed by the masking process with the estimated coil sensitivity map from dual-echo sequence (Fig. 3C). Our masking method using coil sensitivity map was compared to the general high-pass filtering (Figs. D & E) to correct the intensity inhomogeneity. The corrected magnitude image by high-pass filtering of Fig. 3E improved the homogeneity particularly in the right frontal region and basal ganglia area in this sample (Fig. 3F). However, the excessive high-pass filtering can produce the intensity artifacts in the relatively large structures in the brain such as lateral body ventricle (compare white-arrowheads in Figs. 3C & F). (2) *Phase reconstruction* - The susceptibility phase images were compared with two categorized algorithms; (I) *high-pass filtering of summed multi-channel data* (in either phase or complex domain) and (II) *summation of high-passed complex data* (in complex domain). The first category is more sub-categorized into (I-1) summation of unwrapped phase image corrected with system phase map (SUP), and (I-2) simple summation of complex raw data (SC). The second category has (II-1) complex summation of raw data magnitude-weighting (CSMW), and (II-2) complex summation of the coil sensitivity map-weighting (CSSW). The phase by SUP and SC produced the uncorrelated artifacts (i.e., noise & phase incoherence) (see white-arrowheads in Figs. 4A & B). The CSMW method using calculated susceptibility phase & raw-magnitude-weighting, and high-pass-filtering improved the quality of susceptibility phase with less noise and no hypo-intense blob artifacts around the right frontal region (Fig. 4C). The CSSW phase with the sensitivity-map-weighting looks comparable to that of CSMW (Figs. 4C and D). Among these phase methods, the CSSW improved SNR in most (Fig. 4E). As well, the CSSW method overcomes the artifacts in CSMW; particularly in the (almost saturated) low intensity area such as blood vessels (black-arrowheads in Fig. 4F). In conclusion, the proposed algorithm using dual-echo acquisition improved the intensity homogeneity in magnitude image, and removed the phase dislocation with a good SNR in phase image. This technique will be an effective reconstruction method for the high-resolution image at high-field magnet and multi-channel coil system. **[Reference]** 1. Duyn et al., *PNAS*, 2006. 2. Hammond et al., *Neuroimage*, 2007. 3. de Zwart et al., *MRM*, 2002. 4. Wiggins et al., *MRM*, 2005. 5. Ibraham et al., *MRI*, 2001. 6. Wald et al., *MRM*, 1995. 7. Cohen et al., *HBM*, 2000. 8. van Gelderen et al., *ISMRM*, 2006. 9. Roemer et al., *MRM*, 1990. 10. Schofield et al., *Optics letters*, 2003. **[Acknowledgements]** We thank Dr. Z.H. Cho for the support of a 7T multi-channel head RF coil.